Impedance Modeling of Low-Voltage Cables considering Capacitances and Parameter Uncertainty using Finite-Element Method

Max Murglat
Simon Krahl
FGH e.V.
Aachen, Germany
max.murglat@fgh-ma.de

Andreas Ulbig
IAEW
RWTH Aachen University
Aachen, Germany

***Abstract*—Recent research presented methods to improve the calculation of low voltage cable parameters by using finite-element models due to increasing focus on power quality issues in distribution grids. However, the focus was mostly on series parameters and nominal frequency. In this paper the calculation of cable capacitances as well as their impact on harmonic impedance of a single cable and in a rural low voltage grid is discussed using detailed finite-element models. Moreover, the accuracy of geometric simplification was quantified. The results are used to compare and optimize existing analytical equations. Furthermore, sources of uncertainty in cable modeling were identified and their range of impact on impedance was subsequently studied to give recommendations regarding necessary study cases for a robust assessment of grid impedance.**

***Index Terms*-- low voltage cable parameters, grid impedance, power quality, cable capacitance, finite-element**

I. Introduction

The proceeding integration of customers connected to the grid by power electronics, such as photovoltaic systems, heat pumps and electric vehicles, bodes challenges in the scope of power quality in low voltage grids as the level of emitted harmonics is likely to increase [1]. One focus area is the impact of emitted harmonics up into the kHz range, which can lead to undesired voltage distortions, excitation of resonances or stability risks [2]-[4]. An important indicator of potential issues is the frequency-dependent grid impedance [5]. Knowledge of the impedance, including possible resonances, allows an assessment of the expected power losses and risks from harmonics. To comply with existing limits, identify problems at an early stage and plan countermeasures, the trend and phenomena must be appropriately modelled and simulated. Furthermore, considering the switching frequencies of modern inverters, sufficient knowledge of grid properties in the range of supraharmonics will be important [6], [7], where German as well as international standards specify limits and compatibility levels up to 9 kHz [8], [9].

The calculation of the grid impedance necessitates the accurate modelling of the frequency dependent behavior of low-voltage cables, which has thus been of increasing interest in the research. As their frequency dependent behavior is usually not provided by the manufacturer, impedance modeling of cables is subject to specialized studies [6]. There are multiple options for the determination of frequency dependent cable parameters for simulations in the frequency domain. Common simulation software platforms use analytical formulas generally based on equations by Carson or Pollaczek with some modifications. Analytical equations provide a decent balance between accuracy, flexibility and computational burden [10] – [12]. However, when using these equations, it is always necessary to note the underlying assumptions to correctly assess the accuracy of the results. Recent studies have pointed out some drawbacks in analytical modeling, questioning their applicability for low voltage cables as they originally were developed for long overhead lines with underground earth return path [13]. Specifically for multi-core underground cables analytical formulas are given by Ametani, which are based on the assumptions of Wedepohl [14]. However, as no theoretical formulas for the calculation of cable parameters for arbitrary conductor shapes are present, the equations are derived from simplified geometries, i.e. idealized sector shapes and consequent approximations with equivalent circular conductors [14].

There are correction factors, for e. g. the skin-effect, but these are only accurate to a certain degree and generally neglect the actual geometry and lay of the cable. To overcome these errors when calculating cable parameters at higher frequencies as well as benchmarking new analytical formulas, recently finite-element (FE) modeling of low voltage cable has emerged in the literature to achieve a high degree of accuracy [6], [7], [12]-[15].

Many applications of FE models were done in the context of studies concerning nominal frequency, with a focus for example on voltage unbalance [13], [15]. There, the cable capacitances are generally neglected due to short cable lengths of mostly below 1 km for a single feeder, with individual segments often around tens of meters. However, there are no quantifications of the validity of this assumption in the

This research has received funding from the BMWK in Project QUIRINUS-Control (FKZ 03EI4048A)

considered kHz-frequency range for studies concerning harmonic grid impedance. Furthermore, detailed cable models require numerous parameters, which cannot be precisely determined or exhibit significant fluctuations. Moreover, some parameters must be assumed due to manufacturing tolerances or the possible influence of the environment and grid use case. Recent studies have highlighted the importance of considering uncertainties but focused on nominal frequency and assumed uncertainty to be of a certain value [15], [16]. In this paper, the capacitances are calculated using 2D-FE simulations and the impact of possible uncertainties is presented and quantified. The simulations are carried out using the open-source simulation software FEMM, which is built upon Delaunay triangulation, variational formulation, and uses a complex, symmetric biconjugate gradient solver [17]. The 2D approach assumes conductors are infinitely long and parallel and therefore only considers transversal field components. Some studies have pointed out the possible accuracy improvement of 3D models if twisted and magnetic armor is present, i.e. submarine cables [18]. However, this demands an enormous computational burden, and since the considered low-voltage cables have no steel armor, a 3D approach is neglected.

II. FE Modeling of Low Voltage Cables

Commonly used cable types in German low voltage grids are four-core NAYY and four- or three-core NAYCWY with conductor cross-sectional areas of 90, 150, 185, and 240 mm^2 [19]. The conductors can either be fabricated as a single conductor or be composed of multiple smaller subconductors. In the following section, single conductors are assumed to be made of either aluminum or copper. For NAYCWY cable types, the shield (concentric conductor which functions as PE or PEN) is modeled as a single conductor as well. The shield conductor is made of copper.

A. Cable Geometry

The general geometric layout and relevant parameters for a four-core NAYCWY cable are shown in Fig. 1, including the capacitances for one phase and the shield. Reference [12] first provided the formulas to calculate the conductor and cable geometry from the given cable parameters in British standards. The counterparts in the German standard [20] were identified in [13].

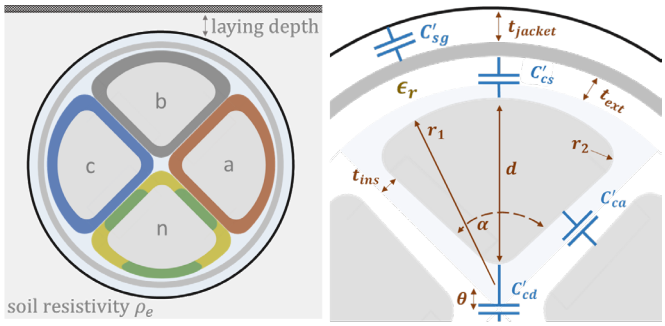

Figure 1: NAYCWY cable: general layout (left) geometric parameters and capacitances (right).

The standard provides values for every necessary parameter, depending on cable type and cross section area. Table I shows exemplary parameters for a 4x185 mm^2 NAYCWY cable. Specific parameters are also provided with a possible deviation from the nominal value, allowing for manufacturing tolerances, e.g., up to 15 % for t_{ins} [17].

Table I: Parameters for a 4x185 mm^2 NAYY cable [20]

Parameter	Definition	Value [mm]	Tolerance [mm]
t_{ins}	Insulation thickness of conductor	2.0	Min. 1.7
t_{ext}	Insulation thickness of common core covering	1.0	-
t_{jacket}	Insulation thickness of jacket	2.7	-
r_1	Back radius	17.8	-
r_2	Corner radius	3.0	-
d	Sector depth	13.8	+/- 0.6
α	Sector angle	90	-

B. Calculation of Capacitances

The relevant capacitances in a low voltage cable can be divided into capacitances between adjacent conductors (C'_{ca}), diagonal conductors (C'_{cd}, only four wire cables), conductor and shield (C'_{cs}), shield and ground (C'_{sg}) or conductor and ground (C'_{cg}). The calculation of capacitances in FEMM as well as similar software can be achieved by exciting one conductor with a specified voltage and setting the other conductors to zero potential [21], [22]. Evaluating the induced charge on every conducting element yields the capacitance (1).

$$[C_{i,j}] = [q_{i,j}/V_j] \tag{1}$$

where $q_{i,j}$ is the induced charge at conductor i from the applied voltage V_j of conductor j, with which the capacitance $C_{i,j}$ between conductors i and j can be calculated.

Generally, this process must be repeated for every conductor to get the whole capacitance matrix. For a NAYCWY cable with four wires, this would necessitate five different simulations. Since the considered cables are rotational symmetrical, this number can be reduced to the minimal number of columns that contain all unique parameters. As shown in the matrix in equation (2) for a cable with a shield, two simulations are necessary while only one simulation must be done for cables without a shield.

$$[C'_{NAYCWY}] = \begin{bmatrix} C_1 & C_2 & C_3 & C_2 & C_4 \\ C_2 & C_1 & C_2 & C_3 & C_4 \\ C_3 & C_2 & C_1 & C_2 & C_4 \\ C_2 & C_3 & C_2 & C_1 & C_4 \\ C_4 & C_4 & C_4 & C_4 & C_5 \end{bmatrix} \tag{2}$$

$$C_1 = 2 \cdot C'_{ca} + C'_{cd} + C'_{cs} \tag{3}$$

$$C_2 = -C'_{ca} \tag{4}$$

$$C_3 = -C'_{cd} \tag{5}$$

$$C_4 = -C'_{cs} \quad (6)$$
$$C_5 = 4 \cdot C'_{cs} + C'_{sg} \quad (7)$$

Simulation of electric fields requires the definition of relative permittivity ε_r in every region. As an insulation material, only polyvinyl chloride (PVC) is considered for all low voltage cable types and every region (conductor, core covering, and jacket insulation) with a nominal value of 4. However, it must be noted that, depending on the exact composition, the nominal value can vary between 3 and 4. Furthermore, the permittivity also depends on the cable operating temperature and increases with temperature [13]. All other conducting materials (copper and aluminum) have a relative permittivity of 1.

It must be noted that this approach assumes the surrounding soil to have zero potential as a boundary condition. While earth is far from being a good conductor, considering the common soil resistivity of 100 Ωm, charges in the earth will still dilute themselves with the small time constant of 10^{-9} s [23]. Therefore, this assumption is plausible for studies concerning steady state models.

C. Calculation of Series Impedance

The determination of series impedance parameters R' and L' is similar to the described process for capacitance calculation. The conductors are instead now excited with a current, and the resulting voltage drop over the conductors allows the extraction of the cable parameters [6], [12]. Again, under the assumption of rotational symmetry, the number of necessary simulations can be reduced to two and one for cables with and without shield respectively [21] .

To carry out the electro-magnetic simulations, all conductor properties must be assigned a relative permeability μ_r and electrical conductivity σ. Since no ferromagnetic materials are used, μ_r is set to 1 for everywhere. The conductivity of the surrounding earth depends on the soil resistivity ρ_e and exhibits a wide range for different environmental conditions [15]. A standard value of 100 Ωm leads to a conductivity of 10^{-8} MS/m. The conductivity depends on the material and is 37 and 58 MS/m for aluminum and copper. Electric conductivity is dependent on temperature and can be modeled with the following equation (8) [13].

$$R'_{DC}(\theta) = R'_{DC}(20) \cdot [1 + \alpha\,(\theta - 20)] \quad (8)$$

The temperature coefficient α is 0.0039 for aluminum and 0.0043 for copper. R'_{DC} is the DC resistance of the conductor and θ the temperature in °C.

The boundary condition for series impedance calculation is a magnetic vector potential A = 0 at a circle with a distance of 80 m from the cable [12].

D. Approximated Geometric Model

As a model simplification of the complex geometry of the conductors as shown in Fig.1, they can also be approximated as thirds or quarters of a circle defined only by their radius and distance from the cable center [15], [21]. In Fig. 2 the results of the complete and approximated model are depicted for a NAYY cable and different cross section areas.

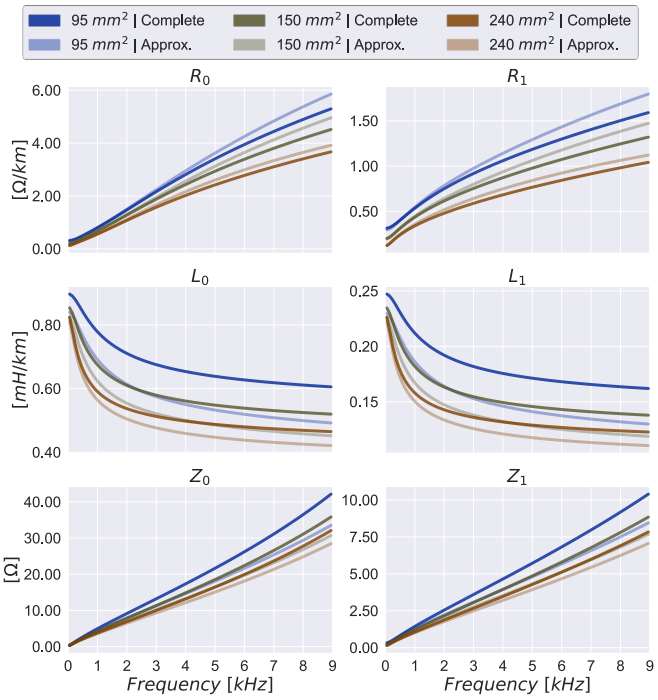

Figure 2: Influence of approximation of conductor geometry on series parameters and short circuit impedance for a NAYY cable with different cross section areas.

While this approximation has little effect on the parameters at nominal frequency the error increases significantly with increasing frequency. For the cable with 150 mm² cross section the error is greater than 10 % at 3150 and 3450 Hz for zero and positive sequence respectively and is around 15 % for both at 9000 Hz.

The current distribution for both cases is shown in Fig 3. The current density is much higher at the sharp edges in the approximated model compared to the smoother edges in the complete model. From Fig. 2 it can be concluded that this concentration of pronounced current hotspots leads to underestimating the resulting inductance, which causes the deviation in the impedance calculation.

Furthermore, the results show that the influence of the conductor approximation increases with decreasing cross section area. The smaller cross section causes the generation of significant current hotspots at earlier frequencies. Comparing the results to a cable with a shield showed that the influence of a shield decreased the error from the approximated geometry, especially for the zero sequence parameters and impedance.

In conclusion, approximating the conductors by a quarter or a third of a circle can be reasonable for studies concerning nominal to low frequencies. However, for harmonic studies in the range of kHz it is necessary to model the cable geometry

as realistically as possible, especially for cables with a small cross section area. Therefore, in the following simplified models are neglected, and the complete model for conductor geometry is used.

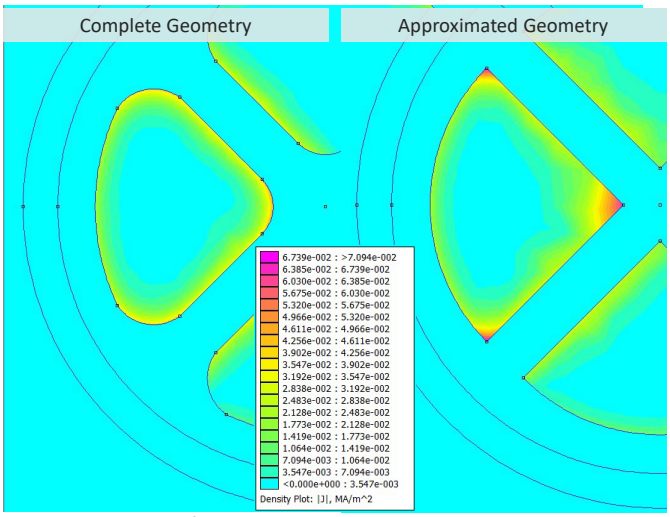

Figure 3: 4x185 mm^2 NAYY cable current density at 9 kHz with complete geometry (left) and approximation by quarter circle (right).

Additionaly, the influence of the laying depth of the cable system was analyzed. Different depths ranging from 40 to 150 cm were considered. The results showed only a very minor influence of laying depth, which is thus fixed to 80 cm in the following.

III. Cable Capacitances

The results of the calculation of the zero and positive sequence capacitances for the considered cable types and cross section areas are depicted in Fig. 4. The results from the FE simulations are shown in bold. The results indicate that the cable type has a strong influence on the positive sequence capacitances and should be considered in detailed harmonic studies.

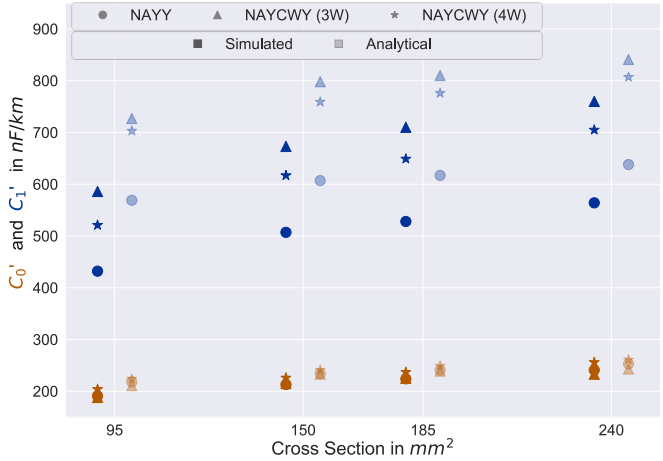

Figure 4: Cable capacitances using FEMM and analytical approximations for positive (blue) and zero (orange) sequence.

The cable without a shield (NAYY) generally presents the lowest values. Increasing the cross section area increases the capacitance. Concerning zero sequence capacitance, the cable type has only a small influence and increasing cross section area increases the capacitance only slightly.

The results from the FE simulations are additionally compared to an analytical approximation (equations (9) – (13), parameters given in Table I). This approximation was first proposed in [21] and assumes the conductors to be fractions of a circle, similar to the geometric simplification presented in section II-D. The general equation for the capacitance of a cylindrical conductor can subsequently be used to approximate the capacitances C'_{cg}, C'_{cs} and C'_{sg} in Fig. 1. The capacitance between adjacent conductors (C'_{ca}) is approximated as a plate capacitor. No equation exists for the approximation of the diagonal conductors (C'_{cd}). Thus, they are assumed to be 5 % of the capacitance of adjacent conductors [13].

$$C'_{ca} = \frac{\epsilon_0 \cdot \epsilon_r \cdot r_1}{2 \cdot t_{ins}} \tag{9}$$

$$C'_{cd} = 0.05 \cdot C'_{ca} \tag{10}$$

$$C'_{cg} = \frac{1}{4} \cdot \frac{2\pi \cdot \epsilon_0 \cdot \epsilon_r}{\ln\left(\frac{r_1 + \theta + t_{ins} + t_{ext} + t_{jacket}}{r_1 + \theta}\right)} \tag{11}$$

$$C'_{cs} = \frac{1}{n_{wires}} \cdot \frac{2\pi \cdot \epsilon_0 \cdot \epsilon_r}{\ln\left(\frac{r_1 + \theta + t_{ins} + t_{ext}}{r_1 + \theta}\right)} \tag{12}$$

$$C'_{sg} = \frac{2\pi \cdot \epsilon_0 \cdot \epsilon_r}{\ln\left(\frac{r_1 + \theta + t_{ins} + t_{ext} + t_{jacket}}{r_1 + \theta + t_{ins} + t_{ext}}\right)} \tag{13}$$

The results of these equations are depicted in Fig. 5. It is observed that these analytical equations overestimate the capacitances by up to 20 %. Taking into consideration the actual geometry of the cable as presented in Fig. 1 and Fig. 3 this can be explained as the conductors are not perfect quarters or thirds of a circle, and therefore the actual error is larger, as was stated in [21], where approximated geometry was used in comparison to the analytical equation. Extending the equation with a correction factor improves the calculations of the capacitances. The value of this factor for cable type and cross section is depicted in Fig. 5. In alignment with the results regarding sequence capacitances in Fig 4 the results show that the simulated capacitances are lower than the analytical values. The error decreases with increasing cable cross section and is up to 30 % for a 95 mm^2 and ca. 15 % for a 240 mm^2 cable for the capacitance between adjacent conductors C'_{cs}. Furthermore, the error differs only slightly for small cross sections with varying cable type.

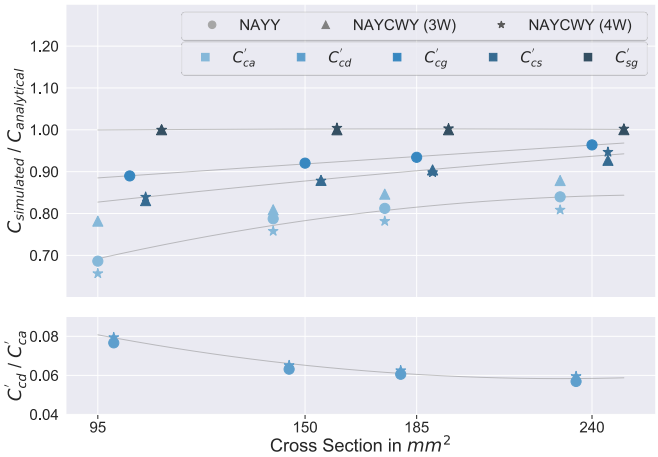

Figure 5: Correction factor accounting for the geometric simplifications in (9) – (13).

Using least squares polynomial regression technique equations for the calculation of the correction factor can be determined. This factor relates the capacitances from the FE-simulations ($C'_{simulated}$) to the results from the analytical calculation ($C'_{analytical}$) using (9) - (13). A quadratic function resulted in a sufficient approximation. This function is shown in (14) and depends only on the cross section A of the cable.

$$k = \frac{C'_{simulated}}{C'_{analytical}} = p_1 \cdot A^2 + p_2 \cdot A + p_3 \qquad (14)$$

where k is the correction factor, p_1, p_2 and p_3 are the coefficients of the quadratic polynomial.
The values for each capacitance are listed in Table II. The resulting functions are shown in Fig. 5 as gray lines. Extending equations (4) – (8) by this factor improves the cable modeling using analytically calculated capacitances.

Table II: Parameters for correction factors

	p_1	p_2	p_3
C'_{ca}	$-4.8 \cdot 10^{-6}$	0.00253	0.5119
C'_{cd}	$1.066 \cdot 10^{-6}$	-0.00049	0.1148
C'_{cg}	$-9.2 \cdot 10^{-8}$	0.00054	0.84
C'_{cs}	$-7.652 \cdot 10^{-7}$	0.00096	0.7516
C'_{sg}	$2.534 \cdot 10^{-7}$	$-9.287 \cdot 10^{-5}$	0.9936

The impact of including cable capacitances in harmonic impedance calculation is discussed in the following using the simulation technique for the determination of cable capacitances.
First, this analysis confirms the assumptions that cable capacitances can be neglected for studies considering grid frequency or the low frequency range or short cables as differences become only visible for cables longer than 500 m and for frequencies above 5 kHz. For the 1000 m long cable the error is greater than 10 % at around 6600 for the zero and 8500 Hz for the positive sequence impedance for the NAYY cable. For the NAYCWY, cable the error is always smaller than 10 % and the maximal error at 9000 Hz is around 6 % and 9 % for the zero and positive sequence impedance. The NAYCWY cable with three wires showed similar behavior to the variant with four wires and is therefore not shown in Fig. 6.

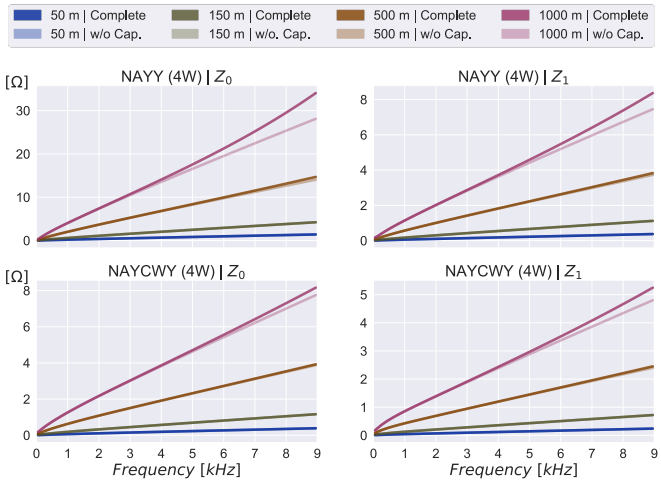

Figure 6: Impact of neglecting capacitances on short circuit sequence impedance for 4x185 mm² NAYY (top) and NAYCWY (bottom) cables with different cable lengths.

Further, for a 1000 m long NAYY as well as a four-wire NAYCWY cable the impact of neglecting the cable capacitances on sequence impedance is shown considering different cross sections areas in Fig. 7.

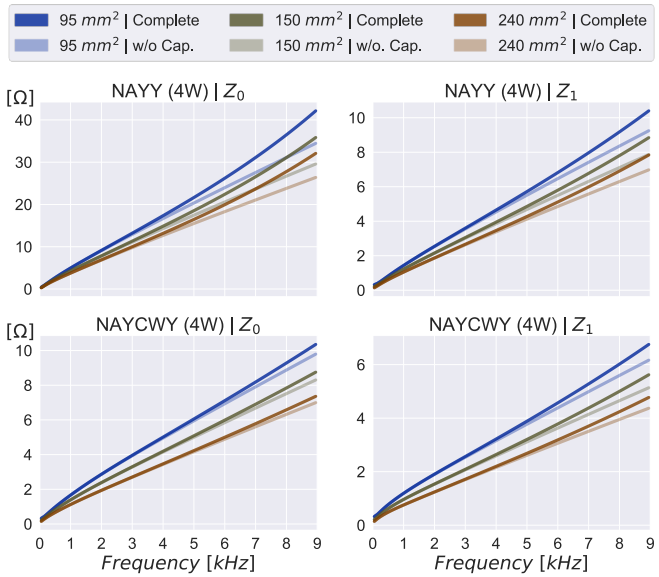

Figure 7: Impact of neglecting capacitances on short circuit sequence impedance for NAYY (top) and four-wire NAYCWY (bottom) cables with different cross sections.

The cable impedances in Fig. 7 indicate that the cross section has no significant impact on the influence of capacitances, as the relative errors are similar for every cross section.

Overall, the results indicate that including capacitance in cable impedance models for harmonic studies is only relevant when frequencies above 5 kHz are of interest, or a high accuracy is desired. Furthermore, for accurate modeling, a distinction between different cable types should be made, as the impedance as well as the impact of neglecting capacitances differ significantly for NAYY and NAYCWY cables.

While these indications and recommendations were derived by analyzing a single cable in detail, an additional study was performed on a low voltage grid to examine the impact of neglecting the capacitances of multiple cables. For this purpose, a synthetic rural grid consisting of six feeders with 127 line sections and a total line length of 2352 m was chosen. The longest line is 140 m long. The grid model includes 153 loads and 43 distributed generation units, which are exclusively PV [24]. Loads were modeled with standard RLC models using power flow data. For the PV generators, only the filter capacitors were considered [25]. To analyze the impact of cable capacitances, all lines were set to the same type, in this case either a 4x185 mm² NAYY or NAYCY cable. Then harmonic impedance calculations were carried out, considering and neglecting the cable capacitances derived from the presented FE simulations.

The results for the positive sequence driving point impedance for two buses located at the start and end of a feeder are shown in Fig. 8. Confirming the previous results, there is little to no impact from including capacitances below 4 kHz. However, a significant difference can be seen at the first parallel resonance at 6 and 6.5 kHz for both buses. Including the capacitances shifts the resonances by 300 and 400 Hz for the two buses, respectively, making modeling of the capacitances necessary for accurately detecting resonance phenomena.

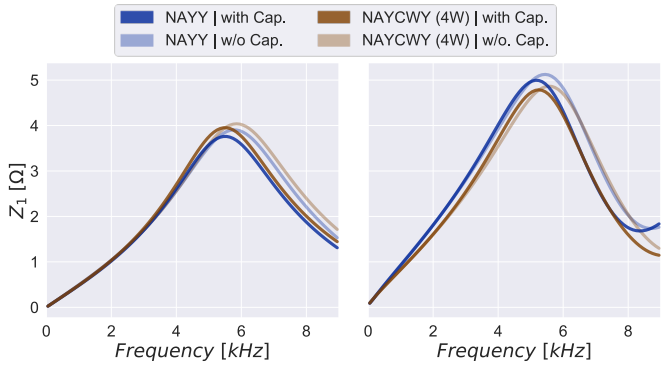

Figure 8: Positive sequence driving point impedance for two buses of a rural grid comparing the impact of neglecting capacitances for NAYY and NAYCWY cables.

Considering the possible shift of several harmonic orders of resonance frequencies including capacitances in low voltage cable models should be advised when analyzing either a high frequency range or if parallel resonances are present in the studied grid.

IV. Impact of Uncertainties

As described in section II, detailed modeling of cables using the FE technique requires assumptions regarding certain geometric or environmental parameters that are subject to aspects like manufacturing tolerances or fluctuations depending on age, season, or grid use case [13] - [16], [20]. In the following section the impact of these assumptions on the cable parameters and impedance is discussed. In Table III, all uncertain parameters considered in this paper are listed.

Table III: Uncertain parameters in cable modeling

Parameter	Unit	Influence		Min.	Nom.	Max.
		Series	Shunt			
Temperature θ	[°C]	X		20	20	70
Soil resistivity ρ_e	[Ωm]	X		30	100	1000
Relative permittivity ε_{PVC}	-		X	3	4	8
Insulation thickness t_{ins} [a]	[mm]	X	X	1.7	2.0	2.0
Sector depth d[a]	[mm]	X	X	13.2	13.8	14.4

a. Values depend on cable type and cross section. Here: 4x185 mm² NAYY

For every uncertain parameter, a calculation with the minimal and maximal possible value, was performed and then compared to the nominal value, while all other parameters remained fixed to their nominal value. The relative change in zero and positive sequence impedance is depicted in Fig. 9 for every parameter in Table III.

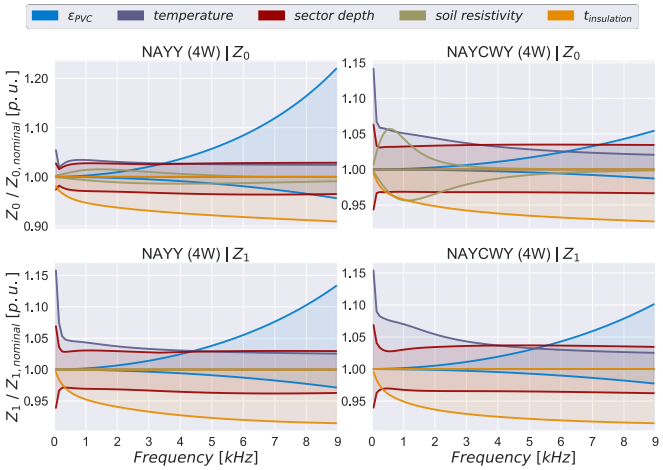

Figure 9: Impact of single parameter uncertainty on the sequence impedance for 4x185 mm² NAYY and NAYCWY cables. Colored areas represent regions from minimum to maximum values.

The results show that all parameter uncertainties impact the impedance, with differences mostly around 5 to 10 % compared

to the nominal value. Overall, it is further evident that the scope of parameter uncertainties depends on frequency. While temperature has the largest impact on impedance for nominal grid frequency, its impact decreases relatively with increasing frequency. Temperature has a major impact on resistance at low frequencies, however, at increasing frequencies, the skin- and proximity effect become more influential, and the overall impedance is dominated by the inductance, which is only slightly affected by the temperature as it increases only by about 2 % for the maximum temperature. In contrast, the relative permittivity has no impact on the low frequency range, because the capacitances of low voltage cables impact the impedance only at several kHz as discussed in section II. However, in the high frequency range, capacitances become a dominant factor and should be modeled accordingly. For the zero sequence impedance, there are also differences in the impact of the uncertainties for the different cable types visible. While temperature and soil resistivity have a larger impact on the NAYCWY cable, relative permittivity is especially impactful for the NAYY cable.

Using the results of the singular parameter uncertainties, scenarios yielding maximal and minimal cable impedance can be defined to quantify the expected range. The necessary value for each parameter is listed in Table IV.

Table IV: Parameter values for extreme impedance scenarios

Scenario	θ	ρ_e	ε_{PVC}	t_{ins}	d
Minimal impedance	min	max	min	min	max
Maximal impedance	max	min	max	max	min

The analysis of extreme scenarios allows a quick assessment of whether critical cases can occur due to parameter uncertainty or whether simplified modeling, e.g., with nominal values, is possible.

The resulting uncertainty for the cable parameters and impedances is depicted in Fig. 10 considering the effect of all parameters, values for the nominal case are given in Table III. Excluding the zero sequence resistance, the overall uncertainties for the parameters are mostly constant over the studied frequency range and in the range of +/- 10 %. If only the nominal values of the respective cable and no detailed and parameterisable model is available, the results suggest that the fluctuations of the positive sequence series resistance and inductance can be assumed to be around this value. Accurate modeling of zero-sequence parameter uncertainty should be chosen according to the cable type. As outlined before, there is an exception at the very low frequency range where temperature is the major influence on resistance and inductance exhibits only minor changes.

Considering the impedance, increasing uncertainty is notable with increasing frequency. This is caused by the increasing influence of the cable capacitances.

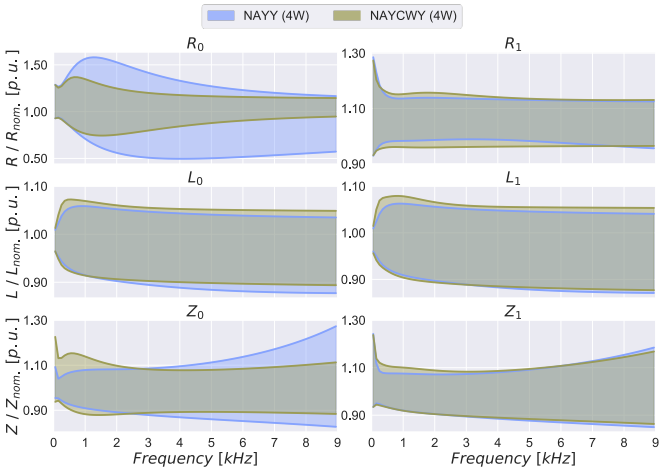

Figure 10: Possible range for cable parameters considering all uncertainties for 4x185 mm² NAYY and NAYCWY cables.

The uncertainty regarding cable capacitances is dominated by the value of relative permittivity which can double the value of the capacitances as a linear relationship is observed. The insulation thickness and sector depth can change the value by up to 12 % and 5 % respectively.

The defined extreme scenarios for the parameter uncertainty were examined in the same rural low voltage grid as presented in section III. The resulting positive sequence is shown in Fig. 11 for the same two buses as previously in Fig. 8.

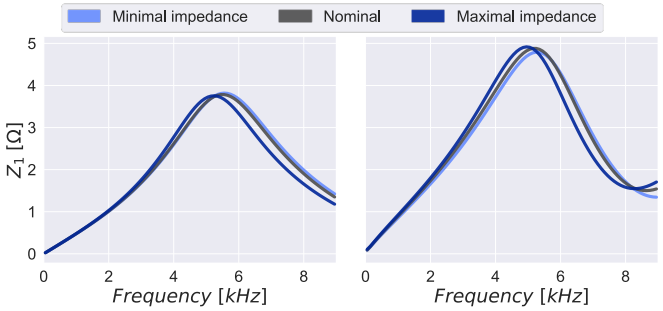

Figure 11: Positive sequence driving point impedance for two buses of a rural grid comparing the influence of uncertainty for a 4x185 mm² NAYY cable.

Analogous to the analysis regarding the impact of the capacitances, little to no influence in the low frequency range is observable. Significant differences become apparent at the parallel resonance, where the resonance frequency is shifted by 300 Hz for the maximal impedance scenario. Thus, assessing possible resonance phenomena should consider uncertainties stemming from cable modeling to accurately evaluate associated risks. In the simplest case, a scenario with nominal parameters and a scenario with maximum impedance should be considered. Further research could focus on defining a probabilistic cable model considering the probability and frequency of the uncertain parameters.

The results show the high relevance of detailed modelling of low-voltage cables. In this context, it must be accentuated that meaningful analyses also require a realistic representation

of the other equipment, e.g. consideration of the frequency-dependent behaviour of transformers due to the skin effect or parasitic capacitances.

V. Conclusion

In this paper, accurate modeling of low voltage cable harmonic impedances using the FE technique was discussed with special focus on the impact of capacitances and sources of uncertainty. A possible simplification of the complex cable geometry showed limitations in accuracy, especially considering higher frequencies, and it is therefore recommended to implement detailed geometric models when studying low voltage cables. The detailed model was used to improve existing analytical formulas for the calculation of capacitances.

Existing assumptions to neglect cable capacitances for the low frequency range were validated. However, grid impedance calculations showed that capacitances can significantly influence the impedance and resonance frequencies at higher frequencies and thus should be included in cable modeling. Furthermore, sources of uncertainty and their influence on the cable parameters were studied. Differences in impedance of up to 10 % for a single cable were observed, which also presented themselves in the shift of several harmonic orders of the resonance frequency in a low voltage grid. Awareness of the dependency of the accuracy on carried out impedance calculations caused by assumptions regarding uncertain parameters is therefore advised.

To validate the obtained cable parameters, measurements should be performed. A measurement procedure with a focus on nominal frequency is presented in [13].

References

[1] M. H. Bollen and S. K. Ronnberg, “Power quality issues in the future electric power system,” Elect. J., vol. 29, no. 10, pp. 49–61, 2016.

[2] J. Meyer, R. Stiegler, P. Schegner, I. Röder, and A. Belger, “Harmonic Resonances in Residential Low Voltage Networks Caused by Consumers Electronics,” in 24th International Conference on Electricity Distribution, 2017, pp. 1–5.

[3] L. Jessen and F. W. Fuchs, “Modeling of inverter output impedance for stability analysis in combination with measured grid impedances,” IEEE 6th International Symposium on Power Electronics for Distributed Generation Systems (PEDG), 2015.

[4] M. Liserre, R. Teodorescu, and F. Blaabjerg, “Stability of photovoltaic and wind turbine grid-connected inverters for a large set of grid impedance values,” IEEE Trans. Power Electron., vol. 21, no. 1, pp. 263–272, Jan. 2006.

[5] L. Jessen, S. Günter, F. W. Fuchs, M. Gottschalk and H. -J. Hinrichs, "Measurement results and performance analysis of the grid impedance in different low voltage grids for a wide frequency band to support grid integration of renewables," 2015 IEEE Energy Conversion Congress and Exposition (ECCE), Montreal, QC, Canada, 2015.

[6] A. Novitskiy, S. Schlegel and D. Westermann, "Positive Sequence Impedances of LV Sector-Shaped Cables in the Frequency Range 2 to 9 kHz," *2021 IEEE PES Innovative Smart Grid Technologies Europe (ISGT Europe)*, Espoo, Finland, 2021, pp. 1-5.

[7] A. Novitskiy, S. Schlegel and D. Westermann, "Zero Sequence Impedances of LV Sector-Shaped Cables in the Frequency Range 2 to 9 kHz," *2021 IEEE PES Innovative Smart Grid Technologies Europe (ISGT Europe)*, Espoo, Finland, 2021, pp. 1-5.

[8] Technical rules for the connection and operation of customer installations to the low voltage network (TAR low voltage), Technische Regeln für den Anschluss von Kundenanlagen an das Niederspannungsnetz und deren Betrieb (TAR Niederspannung) (in German), VDE-AR-N 4100, 2019.

[9] Electromagnetic compatibility (EMC) – Part 2-2: Environment – Compatibility levels for low-frequency conducted disturbances and signalling in public low-voltage power supply systems, IEC 61000-2- 2, 2018.

[10] W. H. Kersting and R. K. Green, "The application of Carson's equation to the steady-state analysis of distribution feeders," *2011 IEEE/PES Power Systems Conference and Exposition*, Phoenix, AZ, USA, 2011, pp. 1-6.

[11] H. Keshtkar, S. Khushalani Solanki and J. M. Solanki, "Improving the Accuracy of Impedance Calculation for Distribution Power System," in *IEEE Transactions on Power Delivery*, vol. 29, no. 2, pp. 570-579, April 2014.

[12] A. J. Urquhart, M. Thomson, Series impedance of distribution cables with sector-shaped conductors, IET Generation, Transmission and Distribution 9 (16) (2015) 2679–2685.

[13] J. Geis-Schroer, S. Hubschneider, L. Held, F. Gielnik, M. Armbruster, M. Suriyah, T. Leibfried, “Modeling of german low voltage cables with ground return path”, Energies 14 (5) 2021.

[14] A. Ametani, T. Ohno, N. Nagaoka. (2015). Impedance and Admittance Formulas. In Cable System Transients: Theory, Modeling and Simulation.

[15] F. Binot, T.D. Le, M. Petit, “Characterization and Modeling of LV Cables Considering External Parameters for Distribution Networks” Energies 14 (23), 2021.

[16] M. Pau, F. Ponci and A. Monti, "Impact of Network Parameters Uncertainties on Distribution Grid Power Flow," *2019 International Conference on Smart Energy Systems and Technologies (SEST)*, Porto, Portugal, 2019, pp. 1-6.

[17] Finite Element Method Magnetics: HomePage. Available online: http://www.femm.info/wiki/HomePage (last accessed on 07 September 2023).

[18] J.C. Del-Pino-López, M. Hatlo, P. Cruz-Romero, “On Simplified 3D Finite Element Simulations of Three-Core Armored Power Cables,” Energies 11(11):3081, 2018.

[19] K. Cibis, "Automatisierte Zielnetzplanung zur Entwicklung von innovativen Planungsgrundsätzen für ländliche Niederspannungsnetze in Europa" Ph.D. dissertation, Bergische Universität Wuppertal, Wuppertal, 2022.

[20] DIN VDE 0276-603 VDE 0276-603:2010-03, Starkstromkabel Teil 603: Energieverteilungskabel Mit Nennspannung 0.6/1 kV; VDE: Berlin, Germany, 2010.

[21] M. Shafieipour, Z. Chen, A. Menshov, J. De Silva, V. Okhmatovski, “Efficiently computing the electrical parameters of cables with arbitrary cross-sections using the method-of-moments”,Electric Power Systems Research 162 (2018) 37–49.

[22] K.K.M.A. Kariyawasam, A.M. Gole, B. Kordi, H.M.J.S.P. De Silva, “Accurate electromagnetic transient modelling of sector-shaped cables.” Proc. Int. Conf. Power Syst. Transients Delft, The Netherlands, (June) (2011) 1–6.

[23] Y. Yin, "Calculation of frequency-dependent parameters of underground power cables with finite element method" Ph.D. dissertation, Dept. Elec. Eng., Univ. British Columbia, Vancouver, 1990.

[24] S. Meinecke, D. Sarajlić, S.R. Drauz, A. Klettke, L.-P. Lauven, C. Rehtanz, A. Moser, M. Braun, “SimBench—A Benchmark Dataset of Electric Power Systems to Compare Innovative Solutions Based on Power Flow Analysis”, Energies 13 (12) 3290, 2020.

[25] T. Busatto, A. Larsson, S. K. Rönnberg and M. H. J. Bollen, "Including Uncertainties From Customer Connections in Calculating Low-Voltage Harmonic Impedance," in *IEEE Transactions on Power Delivery*, vol. 34, no. 2, pp. 606-615, April 2019.